

NANOSIMS-TEM COUPLED STUDY OF THREE HIGHLY SHOCKED L CHONDRITES TO CONSTRAIN THE COLLISIONAL HISTORY OF THE SOLAR SYSTEM. M. Ciocco¹, M. Roskosz¹, B. Doisneau¹, S. Mostefaoui¹ and M. Gounelle¹ IMPMC, CNRS, UMR 7590, Sorbonne Université, Muséum National d'Histoire Naturelle, CP 52, 57 rue Cuvier, Paris F-75231, France. E-mail : marine.ciocco@mnhn.fr

Introduction: Hyper-velocity impacts are a major geological process that shaped the Solar System, and are of prime importance when retracing planetary and asteroidal evolution. In the past decades, several studies aimed at deducing the pressure (P), temperature (T), and particularly the timescales of the shocks. This has been done by studying meteorites, especially L chondrites, which contain abundant shock records such as high pressure minerals (ringwoodite, maskelynite etc...) (trans)formed under high PT conditions in melt veins developed during shock wave propagation [1-4]. The timescales over which the collisions occurred have been estimated through three different methods : (i) crystal growth kinetics [1-3], (ii) chemical diffusion triggered by structural changes of the transformed mineral [2; 4] and (iii) the cooling rates of the veins [5]. However, the inferred shock pulse timescales can vary over several orders of magnitude depending on the approach used, and the estimates based on diffusion studies (e.g. Fe, Mg and Mn distributions) are particularly scattered. NanoSIMS measurements are especially valuable as they allow to perform high-sensitivity chemical mappings over large areas with limited sample preparation compared to TEM. However, the scattering within the different results could possibly arise from analytical artefacts such as insufficient spatial resolution of the NanoSIMS, or from a poor knowledge of diffusion coefficients for the polymorphs of interest. This study aims to determine whether or not NanoSIMS profiles can be used as a reliable tool to infer the shock history of a meteorite by combining TEM and NanoSIMS investigations. Optical, textural, structural and chemical analyses will be presented for three L chondrites.

Methods: Thin sections of Sixiangkou, Acfer 040 and Tenham (3) were first observed with optical microscopy. A Renishaw InVia Reflex Raman microspectrometer was then used to determine the structure of the selected minerals. A laser beam ($\lambda=532\text{nm}$) was focused onto the sample for 5 seconds and with 5 to 20 stacked measurements. Polymorphs' textures were investigated with a Zeiss Ultra55 SEM-FEG. Chemical maps of ^{44}Ca , ^{27}Al , ^{28}Si , ^{23}Na , ^{39}K , ^{55}Mn , and ^{56}Fe were acquired with a NanoSIMS 50 over selected $15\mu\text{m}^2$ to $40\mu\text{m}^2$ areas. A Zeiss Neon40EsB FIB was used to prepare electron transparent sections for Tenham. TEM diffractions, profiles and chemical maps were then collected on a Jeol 2100F.

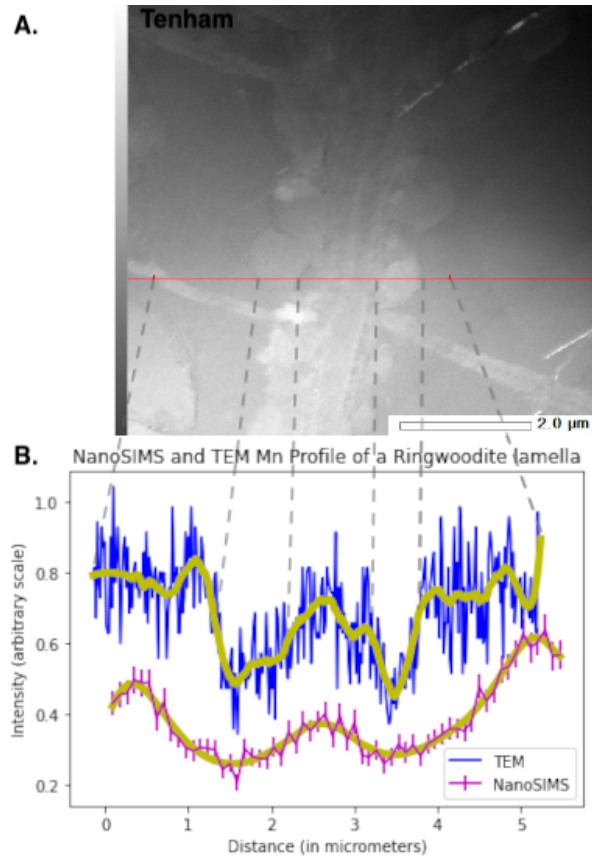


Fig. 1A: STEM image of a ringwoodite lamella 1B: NanoSIMS & TEM Mn profiles of nearby ringwoodite lamellae.

Results: Numerous shocked minerals were detected in all samples, mostly in shock-produced melt veins. Ringwoodite was dominant in all melt veins, whereas maskelynite, akimotoite and pyroxene were always present as minor minerals.

Tenham. The 3 studied sections contain the largest melt areas which enabled us to find numerous remnant olivine bearing ringwoodite lamellae: an assemblage in which redistribution of elements occurs between coexisting crystal structures. Their edges appear jagged on BSE images. NanoSIMS images and the FIB section were collected in the same ringwoodite cross-cut olivine crystal. A TEM investigation reveals that the larger ($2\mu\text{m}$ and over) lamellae are constituted of an inner fine-grained aggregate embedded in a layer of polycrystalline ringwoodite (Fig. 1A). Compositional contrasts between the edges and the centers of the lamellae are shown in Fig. 1B. The outer edge is depleted in Mn and

Mg, and enriched in Fe compared to the host olivine. Conversely, the central part does not show significant depletion in Mn. Straighter, smaller sets of oriented lamellae were also observed. They are $\sim 0.2\mu\text{m}$ wide, texturally homogeneous and Mn-depleted. They present chemical gradients similar to those of the outer layer of the larger lamellae.

Sixiangkou. This section also contains olivine bearing ringwoodite lamellae. However, they probably formed from a process different than those in Tenham. Indeed, SEM images show jagged and discontinuous lamellae, implying that they are fully polycrystalline. They do not present a preferential orientation. In NanoSIMS images, they present the same chemical distributions as those reported in Tenham.

Acfer 040. This sample contains a larger variety of polymorphic textures. Ringwoodite is mostly present as aggregates or iron-rich outer layers of olivine crystals. We report fractional crystallization textures for both olivine and pyroxenes polymorphs, similar to those reported in [6,7]. The MgSiO_3 assemblages are chemically heterogeneous: the glassy material is enriched in Ca, Na, Fe and Mn, and depleted in Mg.

Discussion: Our samples present textural specificities pointing towards a diversity of transformation mechanisms. For the large and heterogeneous lamellae in Tenham, the nucleation process appears to have been twofold. An initial coherent nucleation formed the fine-grained inner part of the lamellae. This was followed by incoherent nucleation of the polycrystalline outer edge. This sequence is similar to what is described in [8], but our observed lamellae are thicker. In Sixiangkou, the lamellae are likely entirely polycrystalline, implying a single-step, incoherent formation mechanism. As evidenced from fractional crystallization textures, crystallization from the melt seems more common in Acfer 040. This diversity of mechanisms may indicate that the meteorites originate from different depths within their parent body or that they recorded different shock events. More importantly, this indicates that a direct measurement of the lamellae width may not always provide reliable estimates of the shock pulse, especially in the meteorites where multiple transformation mechanisms are involved.

In this context, combining these results with chemical profiles of the polymorphs assemblages would help to constrain the pulses. The TEM profiles display several features demonstrating that the chemical patterns observed are indeed driven by diffusion: first, Fe and Mg profiles (not shown) correlate, implying interdiffusion. Second, there is excess Mn at the boundary between the polycrystalline ringwoodite and the host olivine, which is consistent with an outward Mn migration. Finally, the high Mn content of the inner part may

represent Mn trapped during the initial coherent transformation or diffusion of Mn from this polycrystalline layer toward this region. Those diffusion profiles exhibit similar shapes in Tenham with both TEM and NanoSIMS (Fig 1.B). With both instruments, the Mn-rich inner part of the profiles have roughly the same width and correspond to the inner part of the lamella (Fig.1A). This high Mn content also matches that of the host olivine. The outer parts of the profiles exhibit low Mn contents. This depletion is expected because of the incompatible nature of Mn in the ringwoodite lattice. This suggests that the NanoSIMS has the spatial resolution necessary to study these chemical features. Nonetheless, the walls of the NanoSIMS profile are wider than in the TEM profiles. This may either indicate a variability of the crystallization history from one lamella to the other, or a strong effect of the orientation of the 2D section analyzed. This results in an apparent diffusion length $\sim 65\%$ longer on the NanoSIMS profile, which would in turn result in a $\sim 170\%$ increase of the estimated shock pulse. Note that this would result in a variability that is comparable to the accuracy of the timescales estimates available in literature.

Conclusion: Our study makes it clear that the diffusion profiles observed in NanoSIMS are not analytical artefacts, but that orientation and/or microstructural variability may make this method unreliable if used alone. The same conclusion would be drawn in the case of shock pulse determination solely based on the lamellae widths. Comparing NanoSIMS chemical maps with complimentary TEM analyses may help to get a more accurate representation of diffusion in shocked meteorites. Further work is clearly needed. First, a comparison between TEM and NanoSIMS profiles of fractional crystallization structures in Acfer 040 will allow us to better understand the origin and implications of the differences between information derived from these two methods. Second, the study of another series of HP polymorphs (pyroxene-akimotoite) will help to better constrain the shock pulses of individual meteorites to decipher the collisional history of the Solar System.

Acknowledgments: We thank A.Bischoff & A.Rubin for providing samples O.Beyssac, N.Menguy & J.-M. Guignier for their assistance with analyses.

References: [1] Beck P. et al. (2005) *Nature* 435, 1071-1074. [2] Ohtani E. et al. (2004) *EPSL* 227, 505-515. [3] Xie X. & Sharp T. G. (2007) *EPSL* 254, 433-445. [4] Chen M. et al. (2006) *Meteoritics Planet. Sci.* 41, 731-737. [5] Xie Z. et al. (2006) *GCA* 70, 504-515. [6] Miyahara M. et al. (2008) *PNAS* 105, 8542-8547. [7] Feng L. et al. (2017) *Am. Min.* 102, 1254-1262. [8] Kerschhofer, L. et al. (1998) *Min. Mag.* 62, 617-638.